IEEE Access
Multidisciplinary | Rapid Review | Open Access Journal

Received March 21, 2022, accepted April 14, 2022, date of publication April 22, 2022, date of current version May 4, 2022.

Digital Object Identifier 10.1109/ACCESS.2022.3169509

In-Situ Monitoring and Defect Detection of Selective Laser Melting Process and Impact of Process Parameters on the Quality of Fabricated SS 316L

MEHRNAZ MODARESIALAM[1], HAMID ROOZBAHANI[2], (Member, IEEE), MARJAN ALIZADEH[2], ANTTI SALMINEN[3], AND HEIKKI HANDROOS[2], (Member, IEEE)

[1]Faculté des Sciences de Saint Jérôme, Institut Matériaux Microélectronique Nanosciences de Provence (IM2NP), Aix-Marseille Université, 13397 Marseille, France
[2]Department of Mechanical Engineering, Lappeenranta-Lahti University of Technology, 53851 Lappeenranta, Finland
[3]Department of Mechanical Engineering, University of Turku, 20014 Turku, Finland

Corresponding author: Hamid Roozbahani (hamid.roozbahani@lut.fi)

This work was supported by the Hub of Application Laboratories for Equipment Assessment in Laser Based Manufacturing (APPOLO) through the FP7-ICT under Grant 609355.

ABSTRACT Selective Laser Melting (SLM) is an advanced Additive Manufacturing (AM) technique for the 3D printing of metals. SLM process parameters and different types of defects that may appear during the manufacturing process affect the quality of the final product. Setting laser parameters and online defect detection contributes to improving the quality of parts fabricated through SLM technology. In this study, the effect of the process parameters on the properties of the product built by the SLM process was investigated, and an in-situ monitoring platform was developed to detect two types of defects during the SLM process. Different samples were built from stainless steel AISI 316 L powder, utilizing various laser process parameters. Using microscopy imaging technique, the melt structure features of the constructed samples were tested, and the results were analyzed. The dependency of porosity formation on laser process parameters and scan strategy was investigated. Moreover, hardness test was performed for all built samples. The platform developed for in-situ monitoring purposes includes an AM machine equipped with pulsed laser, camera, illumination system, and powerful industrial computer equipped with Cameral Link Adapter, FPGA, and Real-Time (RT) modules. An algorithm was designed using LabVIEW® software based on Particle Analysis (PA) to cease the process in the event of detection of defect in any fused layers. The first defect was caused by changing the laser spot diameter, which altered the energy intensity of the laser on the surface, and the second defect was created by the uneven thickness of powder on the platform. The monitoring system detected both defects and stopped the process immediately according to the designed algorithm. Images were taken from the melting process layer by layer using a high-performance camera.

INDEX TERMS Additive manufacturing (AM), focal point position, in-situ monitoring, laser beam diameter, laser energy density, particle analysis (PA), powder thickness, selective laser melting (SLM).

I. INTRODUCTION

Additive manufacturing (AM), or 3D printing, is emerging as a new industrial revolution [1], [2]. AM is growing rapidly in the market due to its ability to offer rapid prototypes, massive scale production, and customer-oriented designs [3]–[5]. In addition, it provides an opportunity to produce objects with a high degree of accuracy for complex structures and efficient fabrications based on the digital design of a product. The desired object is built layer by layer based on the CAD model's data provided by the STL format., which uses triangle facets to simulate the original model. The STL file is first sliced into separate layers, then hatched to generate scan trajectories stored in another format. Each slice made from the CAD design contains the layer's information to be printed [6]–[8]. The AM machine then follows those scan trajectories to produce the object [6], [9]. There are numerous additive manufacturing technologies and various

The associate editor coordinating the review of this manuscript and approving it for publication was Muguang Wang.

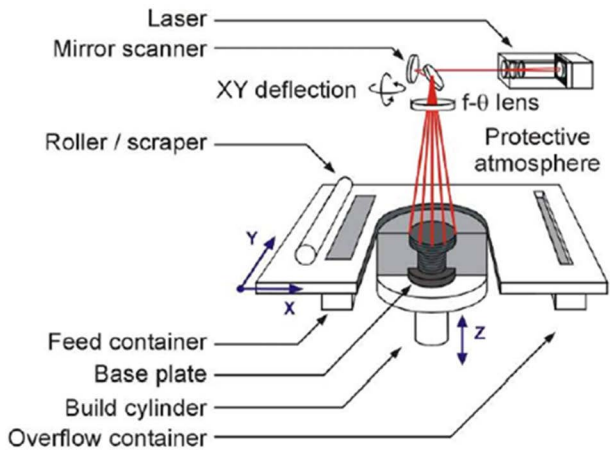

FIGURE 1. Selective laser melting process [20].

materials appropriate for AM processes [10], [11]. Over the past decade, AM has been extensively studied for building metal parts, and novel AM methodologies have been developed for 3D printing of metals with higher accuracy, improved quality, and less processing time [12]–[14]. Various techniques can be utilized for 3D printing of metals, such as Directed Energy Deposition, Laser Powder Bed Fusion (L-PBF), Electron Beam Powder Bed Fusion (EB-PBF), and Binder Jetting [14]–[17]. In this study, Selective Laser Melting (SLM) has been employed. SLM is a type of powder bed fusion additive manufacturing technique and is widely used to create solid objects with complex shapes and special features layer by layer by melting metal powders with a laser beam [18], [19]. Fig. 1 shows the schematic illustration of the selective laser melting process [20].

Although SLM provides unique capabilities in the additive manufacturing of metal products, the quality of components produced by this technology hinders its widespread application in industrial sectors. Laser and material parameters, including the thickness of layers, laser power, laser speed, scanning strategy, hatch distance, and beam diameter, significantly affect the physical and mechanical properties of the metal parts fabricated by the SLM process [21], [22]. Energy density is a determinative factor in the selective laser melting process, but it does not solely specify the shape of the melt pool or properties of the produced part. For example, the porosity of built parts can occur in high and low energy density depending on other factors [22]. Very high energy density can result in keyhole pores or balling effect due to overheating, leading to irregular tracks and geometric surface changes. On the other hand, very low volumetric energy density can be insufficient to melt and solidify the powder [22]. The volume-based energy density E (J/mm3) is defined by Eq. 1, where P is laser power (W), v is scan speed (mm/s), h is hatch spacing (mm) and d is layer thickness (mm) [23], [24]:

$$E = \frac{\mathrm{P}}{\mathrm{v.h.d}} \tag{1}$$

Laser power and scan speed also have a crucial role in the geometric shape of the melt pool. Hatch distance has a great impact on the strength and densification of the SLM-built parts. Moreover, spot size is critical in the laser melting process. By decreasing the spot size, the power density will increase, and the absorption level changes. For maximum penetration, the focal point is located within the workpiece up to a certain depth diameter. In addition, laser scan strategy affects the thermal gradient, ultimately the microstructure and mechanical properties of SLM-built parts. Scanning strategy plays a remarkable role in the formation of defects such as balling effect or high residual stress [25]. Proper selection of scanning strategy increases the uniformity of temperature distribution and improves the properties of the 3D printed product [25], [26]. Inappropriate laser parameters degrade the quality of parts by forming pores, causing cracks, or rougher surface. Furthermore, the defects that occur during the SLM process can cause parts' failure or hamper their performance. One approach to improve the quality of products fabricated by SLM technology is process monitoring and online defect detection. In this way, the defect can be identified in the earliest possible stage, and control measures can be taken subsequently before influencing the properties of the final parts [27], [28]. There are different types of methods and sensors for monitoring the SLM process, such as acoustic, optical, thermal, and vibration systems. For online monitoring of the SLM process, optical-based image processing is the most common method. [29]. Optical sensors have improved significantly during the past years, from simple sensors such as photodiodes to advanced digital cameras, which, when coupled with an illumination system can provide high-resolution images at high speeds to be analyzed through image processing unit [30].

In this study, different cube samples from stainless steel 316 L powder have been produced by applying various SLM process parameters. The structure and melting features of the samples were investigated through an electron-microscope imaging machine. Also, the hardness strength of the samples was evaluated via a hardness test. Moreover, an in-situ monitoring platform has been developed to detect defects that may arise in any fused layer. The optical system has been used for this purpose. AM machine was equipped with a pulsed laser, camera, illumination system, and industrial computer PXI system equipped with Cameral Link Adapter, FPGA, and Real-Time (RT) modules. Using LabVIEW® software, an algorithm has been designed to stop the process if a defect was detected in any fused layers. The working principle of the algorithm is based on Particle Analysis (PA). Since the waiting time for any defects to naturally appear was very long, two types of defects were caused deliberately to evaluate the performance of the developed system. The first defect was caused due to the change in laser spot diameter, which varied the intensity of the laser energy on the surface, and the second defect was caused due to the unevenness of the powder thickness on the platform. Using a high-performance camera, the melting process

was photographed and analyzed layer by layer. If no defect was found, the machine carried on the process. However, in case of detection of any defect by the system, the algorithm stopped the process and did not start forming a new layer. Also, it sent an alarm to inform the operator about the defect. After resolving the cause of the defect, the operator started the machine manually, and the monitoring platform continued working again.

A. BACKGROUND STUDIES

Numerous studies have been conducted on the SLM process. The influence of changing the laser process parameters on the mechanical properties and quality of parts produced by AM process has been investigated in a wide range of studies. Also, the importance of SLM process monitoring and real-time control of defects has been highlighted in recent years, and numerous research efforts have addressed this issue as a high priority research target. Over time, research studies in this field have become more comprehensive, especially with the development of Artificial Intelligence (AI) and machine learning.

Zhang *et al.* analyzed the mechanisms of defect formation in the selective laser melting process. The impact of process parameters, including laser power, hatch space, scan speed, scan strategy, and layer thickness on the formation of defects such as cracks, spherical pores, and irregular fusion holes was investigated. It was shown that energy density is a deterministic factor to control the creation of defects, and scan strategy has an important role in the distribution of defects. Also, the effect of defects on the mechanical properties of the manufactured parts, especially fatigue strength, was discussed. Some strategies for removal and control of defects were proposed based on the analysis performed [31].

The impact of SLM process parameters on the quality of parts was investigated by Maamoun *et al.* A design of experiment was used to analyze porosity, surface roughness, relative density, and dimensional accuracy concerning the interaction between the process parameters. A range of SLM process parameters to obtain optimum performance characteristic values of AlSi10Mg and Al6061 alloys was specified. Also, to demonstrate the interrelationship between relative density, surface topology, dimensional accuracy, and optimal processing window was developed for each material to obtain the final product with high-quality [32].

Utilizing normalized process maps, Bajaj *et al.* proposed a novel approach for rapid process development for the SLM process by identifying a wide processability window for achieving minimum porosities in molybdenum and aluminum. They used plots of normalized energy density vs. normalized hatch spacing and statistical Design of Experiments concept for the development of process parameters such as layer thickness, hatch spacing, exposure time, and point distance. The effectiveness of their proposed method for mentioned metals was proved by achieving relative densities of 97.4% and 99.7% using 200 W pulsed laser and 400 W continuous laser, respectively [33].

Greco *et al.* investigated the SLM process with varying laser power, layer thickness, and hatch space to fabricate AISI 316L. They kept the input energy density constant by adjusting the scanning speed and evaluated varied parameters at two different energy densities. The results showed that different roughness, density, and microhardness were obtained using constant energy density with varying laser parameters. Also, it was shown that the density and the microhardness of the final product could be enhanced by adjusting laser power, the hatch space, and the layer thickness. Moreover, it was demonstrated that the microhardness of the part produced by the SLM process correlates with its relative density. Relative densities up to 99.9% were obtained in the presented study [34].

In contrast with conventional approaches, Barua *et al.* presented a model, which does not involve the melt pool for defect detecting in the laser metal deposition process. They established a vision system to detect thermal irregularities in the laser metal deposition process using an SLR camera to take pictures of the deposited track behind the melt pool. The temperature of the picture's pixels was estimated using radiant surface temperature and calibrated RGB values. Defects were identified through deviation from the reference cooling curve. Residual values were calculated applying linear least squares curve fitting. Porosity defects and cracks were simulated during the laser metal deposition process, and a defect detection model was developed [35].

Tapia and Elwany reviewed the studies in the field of process monitoring and real-time control of additive manufacturing. They addressed the achievements and deficiencies in this field up to the time of their research. Also, various types of sensors and systems developed for monitoring and control purposes were discussed. Moreover, the type of process and type of material involved in each literature were considered in this study [36].

In the study performed by Grasso *et al.*, a method for spatial identification and detection of defects for selective laser melting was proposed. They used a machine vision system for this purpose. Principal Component Analysis (PCA) applied to image data was used to define a statistical descriptor. Defective areas of a layer were recognized precisely using this method. Also, image k-means clustering analysis was performed for the automatic detection of defects. A real case study was investigated to show the effectiveness of the proposed method [37].

In the study conducted by Malekipour and El-Mounairy, typical defects and their contributing parameters were identified and categorized on the powder bed fusion process. They also investigated defects and contributing parameters from the manufacturing features side for monitoring and control purposes to achieve a part without defects. Categorization was performed based on three criteria. All the defects created during the process were involved in the first criteria. Basic parameters for major defects were covered in the second criteria, and the defects that should be recognized by available monitoring approaches to be controlled via standard process

parameters were involved in the third one. Also, an indirect method to control the process was presented [38].

Lane *et al.* used multiple sensors, including a high-speed visible camera, a synchronized thermal camera, and a photodetector to synchronous observe the melt pool and measure a laser powder bed fusion (LPBF) built product with an overhang structure. Using joint-time frequency analysis, the photodetector signal was analyzed. To relate observations from each camera, all acquired signals were synchronized and viewed in a single merged video. Residual heat and slower cooling rates were noticed after forming the melt pool and leaving the overhang edge. The authors found a strong correlation between the photodetector signal and the motion and position of the melt pool according to the scanning strategy. Also, they figured out a possible association between the position of the melt pool dependent on the photodetector field of view [39].

Demir *et al.* proposed a coaxial configured multi-sensor monitoring system for SLM of a tool steel with low processability to monitor process emission and back-reflected laser light. Using a flexible monitoring system with multiple sensors, a better comprehension of the process and means for signaling the defect formation could be provided. Three channels were employed in the monitoring module to simultaneously follow different phenomena. Two digital cameras and a photodiode were used to observe different wavelength bands. The authors considered temporal, spatial, and wavelength bandwidth resolutions in choosing the sensors. They showed the effectiveness of the developed monitoring system with experimental methods and identifying the process transitory concerning thermal stability, laser absorption, and porosity formation [40].

Remani *et al.* demonstrated a multi-sensor approach to correlate the layer-by-layer development of the final part built by metal laser powder bed fusion (MLPBF) with its mechanical properties. The in-process measurements were conducted, and the detected defects were compared with the defects that exist in the finished part. The process was monitored using three sensing systems including multi-view fringe projection, IR thermography, and high-speed thermal imaging technologies to detect the defects as they appear within the final part. Different sensors were used to individually image each layer of the build immediately after completing the laser melting. Using X -ray computed tomography the final part was scanned to evaluate the defects in the part. Using in-process and XCT data, the mechanical assessment was performed to discriminate harmful defects from neutral faults [41]

Song *et al.* proposed a method based on machine learning to monitor the AM process. They used an operating parameter conditioned support vector regression (SVR) method to attain in-situ composition prediction independent of processing parameters. In order to train the SVR, spectral line-intensity-ratio and spectral line-intensity-ratio, and spectral integrated intensity were utilized. For comparison, composition measurements using a calibration curve method, artificial neural networks, and partial least square regression were also conducted. Compared with the other methods, it was shown that the SVR with both input types provides the best performance [42].

Bartlett *et al.* used full-field infrared (IR) thermography to develop an in-situ monitoring system to detect defects and monitor AlSi10Mg specimens during SLM production. They performed transient thermal modeling to support their observations. Ex-situ scanning electron microscopy (SEM) was used to characterize parts to validate data identified defects. The results showed that defects could be identified effectively using the IR defect detection method with an 82% success rate for lack of fusion (LoF) defects. It was also demonstrated that the introduced method has the capability to analyze the presence of systematic process errors during SLM process [43].

A defect detection method for the SLM process using a microphone based on a deep belief network (DBN) was introduced by Ye *et al.* The acoustic signal was processed for quality monitoring for five melted states without signal preprocessing and feature extraction. The results approved the effectiveness of the acoustic signal and DBN method to achieve a high defect detection rate [44].

Liu *et al.* proposed a real-time monitoring system to identify errors automatically using principal component analysis and a support vector machine. A CCD camera captured the molten pool images of the laser AM process, and ten features were obtained. The dimension of the feature set was reduced using the principal component analysis method. The quality of additive manufacturing parts was evaluated by applying a support vector machine model. The results demonstrated that the applied method could achieve a high defect detection rate for two kinds of defects: bulge and slag inclusion [45].

Yadav *et al.* reviewed different types of defects of the SLM process that can be monitored and detected in real-time using in situ sensing sensors based on various machine learning approaches. They reviewed the complexity of the laser powder bed fusion (L-PBF) process, melt pool signatures, in situ monitoring systems, post-processing of in situ sensing data, and automatic detection of defects using machine learning. Different machine learning approaches were reviewed and discussed. The final purpose of the study was to develop a closed feedback control system for real-time quality control and improvement of the L-PBF process [29].

II. EXPERIMENTAL PROCEDURE

Equipment for selective laser melting developed for this research includes a laser system, camera, camera adapter, and an illumination system, which all are connected to the AM machine [46]. Fig. 2 illustrates the schematic diagram of the SLM system of this study. High accuracy, meaning $\pm$ 20-50 μm for small parts and $\pm$ 0.2% for large parts, can be obtained using this machine.

The material used in this process is EOS stainless steel 316 L. Material composition is shown in Table 1 [47].

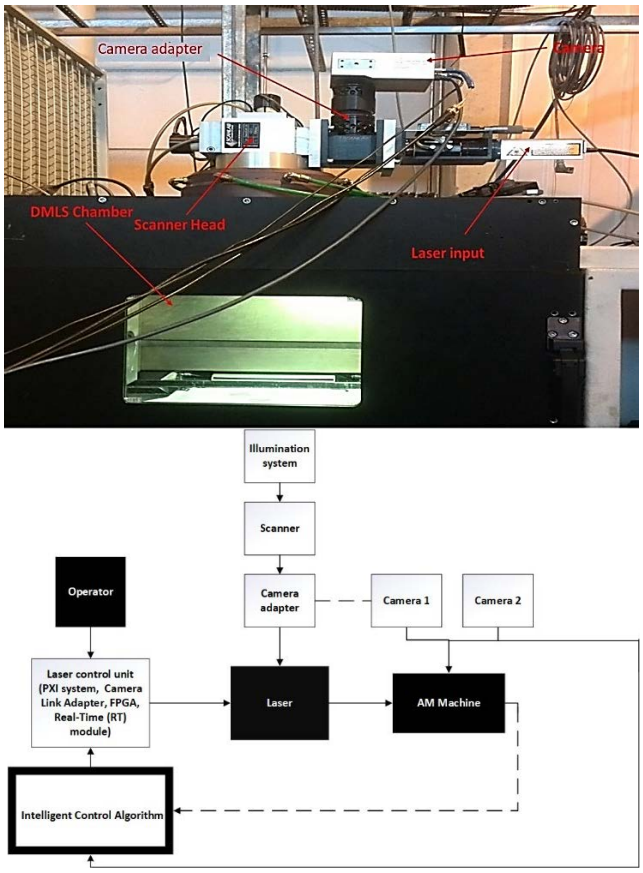

FIGURE 2. Picture of the experimental equipment and its schematic diagram.

TABLE 1. EOS stainless steel 316 L material composition [45].

	Min	Max
Fe	Balance	Balance
Cr	17	19
Ni	13	15
Mo	2.25	3
C		0.030
Mn		2
Cu		0.50
P		0.025
S		0.010
Si		0.75
N		0.10

The additive manufacturing machine used in this research is EOSINT M 270 with Yb: YAG fiber laser, continuous wave (CW) with the wavelength of 1064 nm. This machine has the ability to build parts with a volume of 250 mm $\times$ 250 mm $\times$ 215 mm with a speed of 2-20 mm^3/s depending on the material [48]. Argon gas was used as the shielding gas in the atmospheric pressure inside the machine to minimize oxidation and reduce the weakening effect of the laser beam by the plasma. The high-performance Baumer camera, type TXG14 with Telecentric 55 mm lens equipped with CCD sensor, and Optronis camera model CR3000 $\times$ 2,

TABLE 2. Laser process parameters of built cubes.

	Cube 1	Cube 2	Cube 3
Laser power	200 W	100 W	200 W
Scan speed	1000 mm/s	1500 mm/s	1500 mm/s
Hatch distance	0.1 µm	0.01 µm	0.04 µm

with the full resolution of 1696 $\times$ 1710 pixel, the Global type shutter and the power of 12 W, and the camera adapter installed between the scan head and laser flange, were used for observation of the melting process. In addition, the high-performance pulsed diode laser light source CAVILUX HF with power up to 500W and wavelength of 810 nm was used as the illumination system. NI PXI system, which is equipped with Camera Link Adapter, FPGA, and Real-Time (RT) modules, was chosen for executing image processing and analysis.

Three sample cubes were built using different processing parameters and chessboard scan strategy, as presented in Table 2. The layer thickness is 20 μm. Process parameters have been determined so that do not result in a keyhole melting regime, ensure the stability of scan tracks, and produce high-density samples. Also, since the high energy of the laser can lead to the formation of a plasma plume above the melt pool, the beam parameters were chosen in such a way to keep the line energy regime low, which reduced the plasma formation. The parameters were selected based on the laser power range of 50-300 W, the scanning speed range of 500-2000 mm/s, and the hatch distance range of 0.01-0.2 μm.

All built samples were tested to evaluate their structure and mechanical hardness.

III. MECHANICAL PROPERTIES

A. STRUCTURE TEST

The structure of the material is affected by heating temperature and the thermal cycles of the SLM process. In order to perform the structure experiment, three constructed cubes were cut perpendicular to the build direction, and the cut surface was polished and then washed with the alcohol and dried. In the next step, images from the surface of cubes were taken using microscopy imaging technique to recognize the important changes and the effects of parameters on the cube structure. The imaging tool employed for this purpose was a PME model of Olympus Inverted Metallurgical Microscope. Fig. 3 a), b), c) show the structure images of cubes 1-3, respectively. Fig. 4 a) and b) display scan strategy and melting feature of cube 2 and 3. It should be noted that Fig. 4 shows the top surface of the constructed cubes (no polished cross-section as in Fig. 3).

As shown in Fig. 3 b), the gaps between the molten tracks are visible in cube 2, which were caused due to the low density. In cube 3, small pores were generated, and a good overlapping was achieved, as presented in Fig. 4 b). The heat treatment has an impact on the porosity formation and

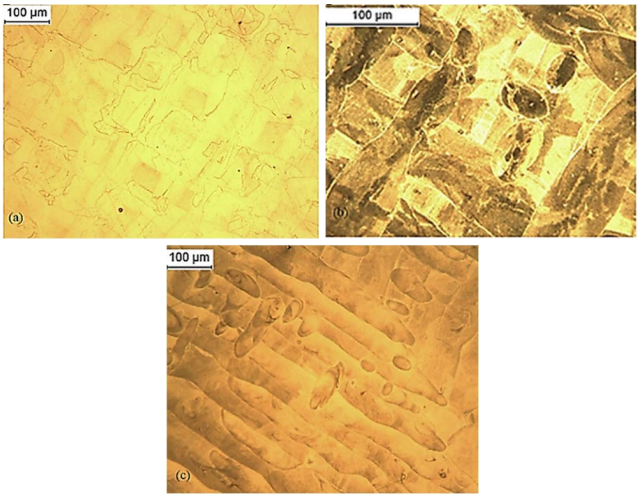

FIGURE 3. Structure a) Cube 1, b) Cube 2, c) Cube 3.

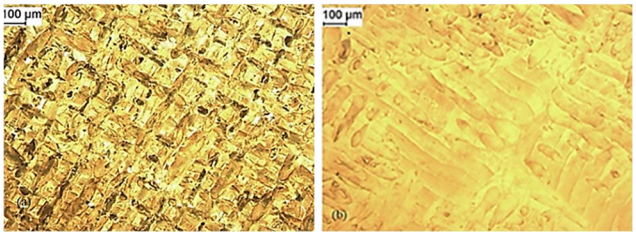

FIGURE 4. Scan strategy and melting feature, a) cube 2, b) cube 3.

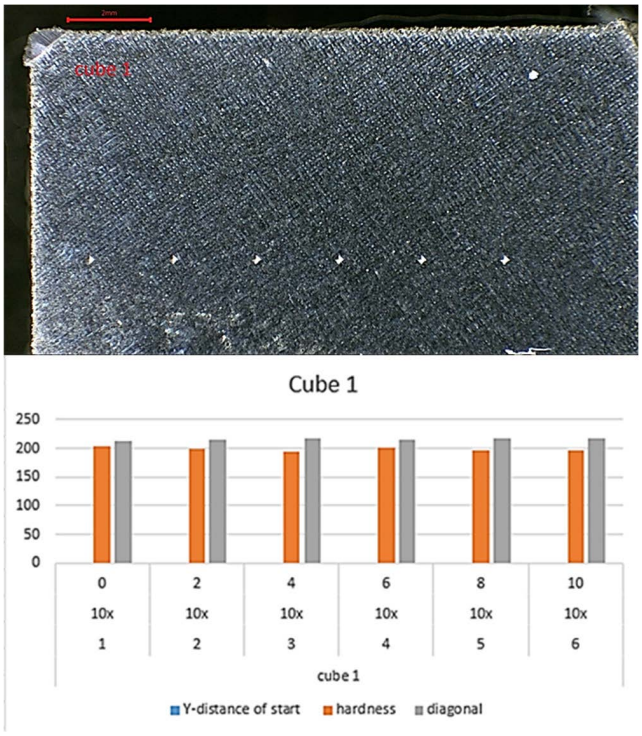

FIGURE 5. Hardness test and measurement graph of cube 1 [46].

densification properties. In general, keyhole pores are formed at high energy density or overheating, thus high laser power and low scanning speed. Porosity varies by various parameters such as scanning speed, laser power, hatch distance, and scan strategy [49], [50]. Loss of overlap between the tracks causes higher porosity. If laser power is constant, the smaller hatch distance nullifies the effect of scan speed on creating the pores. As shown in Fig. 4, the overlap for cube 3 is four times inferior to cube 2. Moreover, in cube 2, a narrower line has been formed in the melting region due to lower laser power. Due to the high cooling rate in the SLM process, a very fine structure is generated. The thermal gradient leads to the thin structure of the melt pool. Enhanced hardness is the result of various factors related to the refined structure.

In this research, one of the crucial points to consider is the temperature changes and heat flow during the process. The temperature during the process affects the solidification morphology in tracks. During solidification in the SLM process, temperature gradient (G) influences the neighboring solid interface. The temperature gradient and the growth rate (R) have a critical role in the microstructure solidification morphology. By changing in scanning speed and the angle of interaction between the laser beam scan track and the growth direction of the solidified material, the growth rate can be modified [51]. Decreasing growth rate at constant temperature gradient leads to a fixed, stable planar consolidation front; however, increasing growth rate results in the cellular formation and dendrite solidification morphologies [52]. The cooling rate is obtained from multiplying $G \times R$, which describes the relationship between the product and microstructure quality, in the sense that a higher value causes a finer microstructure. On the other hand, a high ratio of G/R means more planar stability in front crystallization; hence, a low ratio of G/R makes instability. Moreover, the orientation and amount of the thermal gradient affect the neighboring scan track on the melt pool. Therefore, solidification results vary depending on the changes in G and R [52].

B. HARDNESS TEST

Hardness and tensile strength are major factors in evaluating the mechanical characteristics of manufactured parts [49]–[51], [52]. After polishing and putting in acid, a hardness test was conducted for all produced cube samples utilizing Struers DuraScan 70 hardness tester with Vickers HV5 test method. Hardness tests were done on the surfaces in 6 different points of the cubes. Fig. 5-7 show the hardness test and measurement results for cubes 1-3, respectively [46].

According to the hardness test results, cube 1 and 2 have the same hardness features diagonally; however, the hardness from other points is different for these cubes. Scanning speed and hatch spacing significantly influence the porosity of SLM-built parts. As the porosity increases, hardness, tensile strength, and yield strength of the parts decrease [53]. As the hatch distance and scanning speed increased, the hardness decreased. Moreover, the density of the final part is affected by hatch spacing, scanning speed, and laser power.

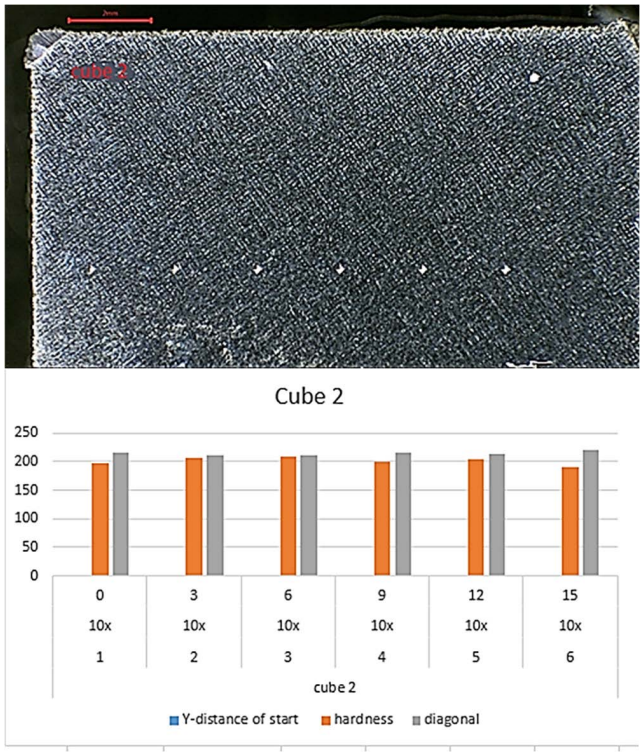

FIGURE 6. Hardness test and measurement graph of cube 2 [46].

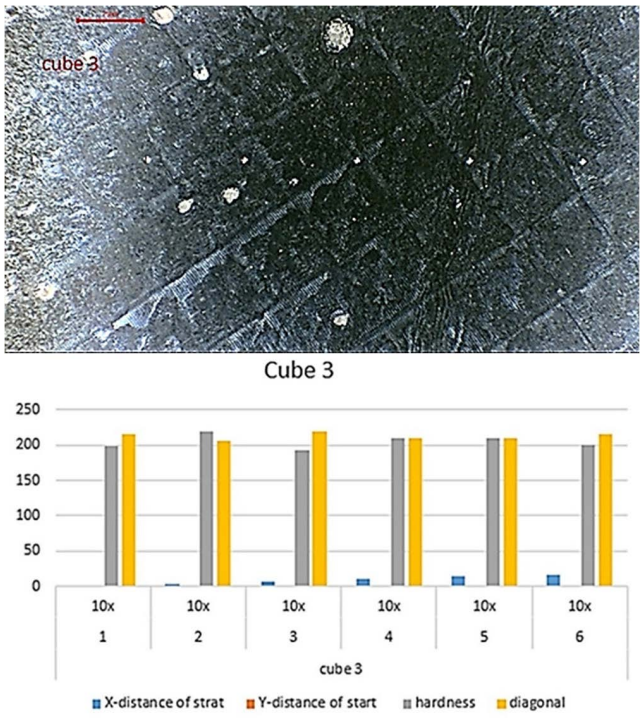

FIGURE 7. Hardness test and measurement graph of cube 3 [46].

Densification can be considerably reduced due to insufficient melting of the powder and the presence of pores caused by improper setting of hatch distance, scanning speed and laser power [53], [54]. Porosities result in the initiation of cracks, low relative densities, and consequently lower hardness of the components.

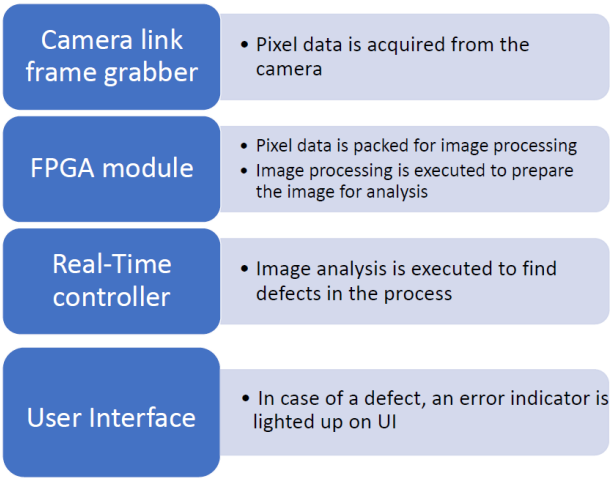

FIGURE 8. Image acquisition and analysis process.

IV. IN-SITU MONITORING

Since the occurrence of any defects in any fused layers can affect the structure of the final product and deteriorate the quality of part, it is important to monitor the process in each layer to detect the possible defects arise during the process. In this study, an in-situ monitoring platform was developed, which aimed to detect the defects that may appear during the SLM process. An algorithm was designed that stops the process immediately if a defect was detected in a layer. The algorithm works based on Particle Analysis (PA), the principle of which is based on the number of particles. The algorithm was developed using LabVIEW software. Fig. 8 shows the pattern of the process of image acquisition and analysis [27].

Through Camera Link cables the acquired image data from the camera is delivered to the Camera Link module and transformed into pixels, which can be manipulated on a computer. The maximum frame rate is 500 frames per second because of the speed of the image processing algorithm; however, in this process, analyzing one image at the end of each fused layer also is good enough. Camera output was set to 10-tap mode, which allows parallel acquisition with ten pixels. The pixels are written into small FIFOs. Image acquisition is controlled by data acquisition state machine with the aim of acquiring the image from the camera only when the image is ready for acquisition. The state machine sends the image information and acquisition status to the User Interface (UI). The 80-bit data is transferred from Cam Data FIFOs to packer CLIP (Computational Linguistics and Information Processing) and converted into eight different FIFOs with 8-bit words through multiple data packing units. The 8-bit data is converted into a Pixel Bus format for thresholding operations, which is then written to Host FIFOs to transfer data from FPGA to Real-Time (RT) controller [27]. The minimum particle size is set

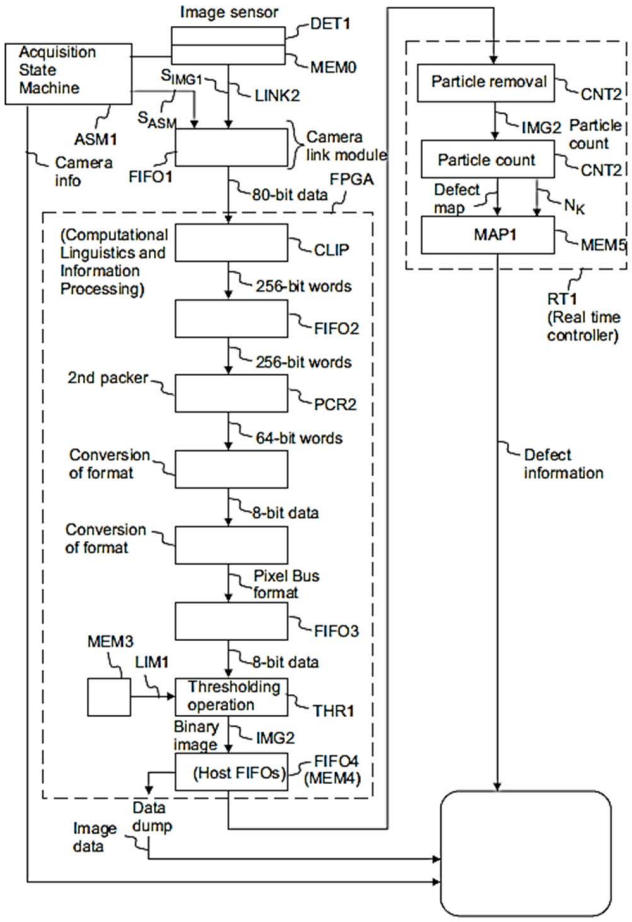

FIGURE 9. Functional units of the data processing system.

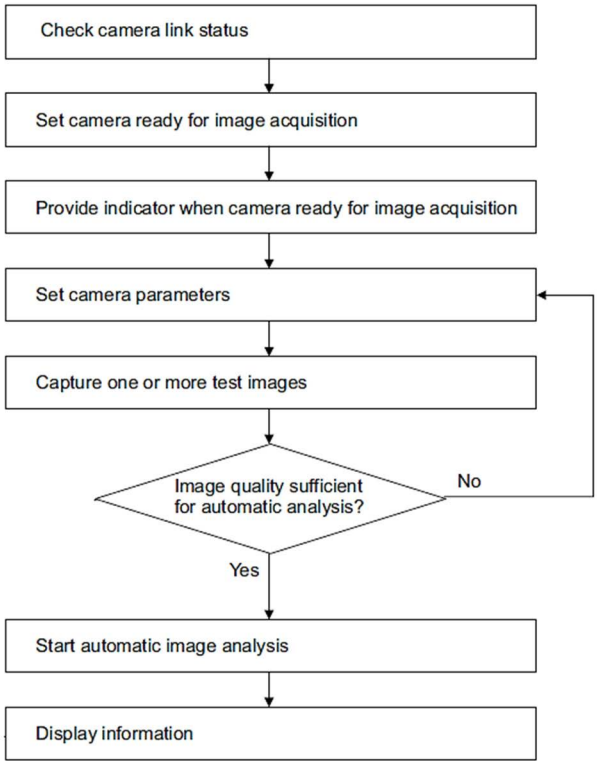

FIGURE 10. Method steps for initializing the automatic image analysis.

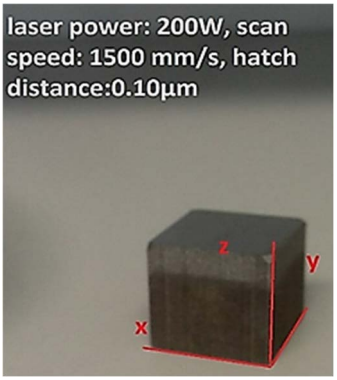

FIGURE 11. Cube sample to test the in-situ monitoring system [46].

to 3×3 pixel. The real-time controller is configured to remove unwanted smaller particles before starting the image analysis. The number of particles of the image is calculated by the real-time controller and returned to the user interface (UI). In case of a defect, the error information is sent to UI. Data delivery from the industrial computer (PXI system) to the PC and vice versa is performed via an Ethernet connection. Fig. 9 displays the data processing system.

Fig. 10 shows the method steps for initializing the automatic image analysis. As the waiting time for any defect that appears naturally was too long, therefore two types of defects were caused intentionally in order to evaluate the performance of the developed system. The first defect was caused by changing the laser spot diameter, and the second one by creating unevenness in the layer's thickness. The monitoring system was tested for both defects to ensure that it could detect the defects and react according to the developed algorithm. After forming each layer, an image was taken and analyzed, and in case no defect was found then the machine continues the SLM process. If the system detects any defect, the algorithm stops the process, and does not start forming a new layer. It also sends an alarm to the UI to inform the operator about the defect. After eliminating the cause of the defect, the operator can manually return the machine to carry on, and the monitoring platform continues to control the quality of the new layers in real-time.

Another cube was created with laser power of 200 W, a scan speed of 1500 mm/s, and a hatch distance of 0.10 μm for the defect test. Fig. 11 illustrates the final produced cube [46].

A. LASER BEAM DIAMETER CHANGE

The laser beam diameter on the powder bed determines the energy intensity, which affects the depth of laser beam penetration. Declining the spot size results in increasing the energy density by the proportional value of $1/e^2$. Beam

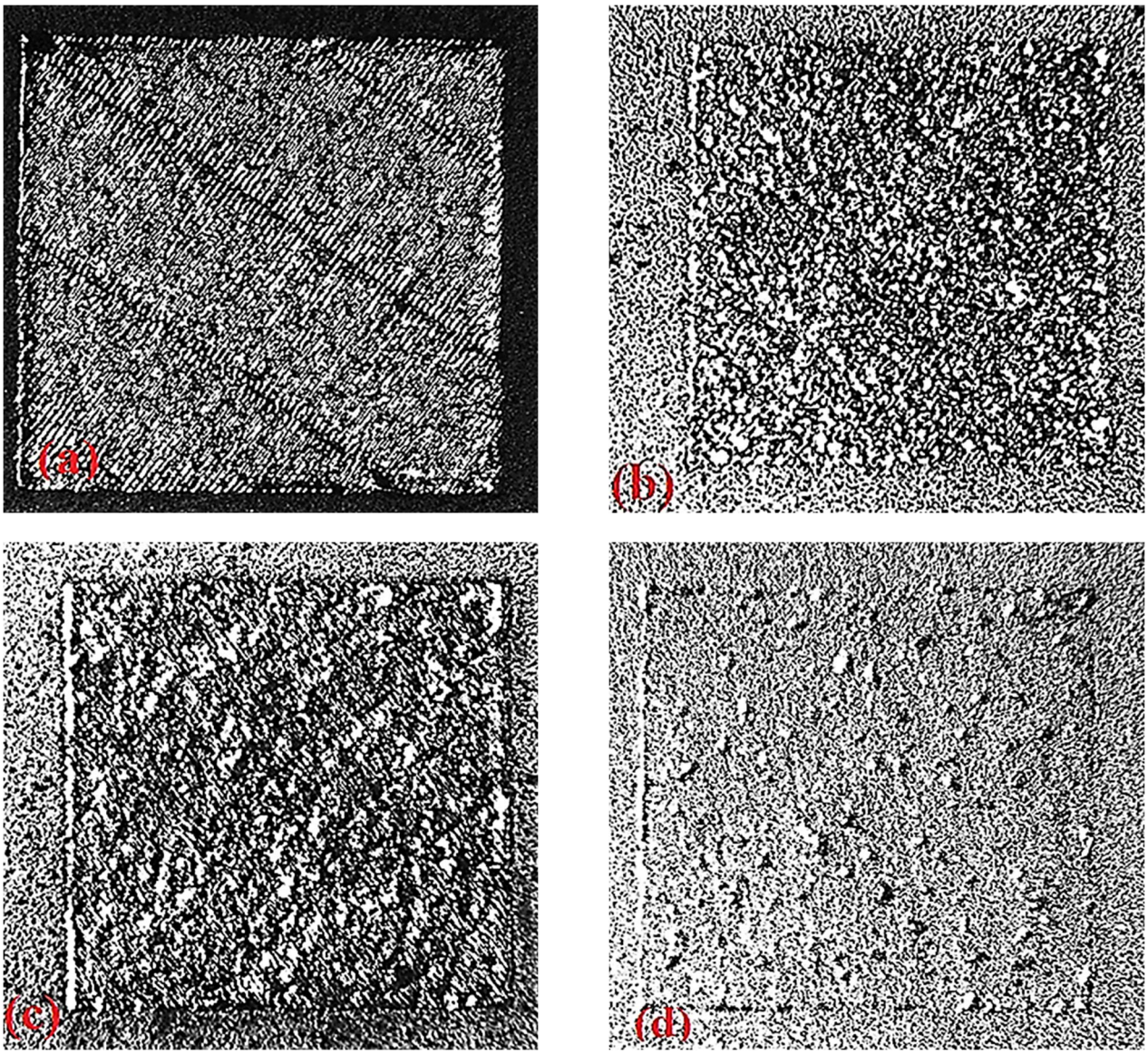

FIGURE 12. a) Completed layer before changing the laser beam diameter b) In-situ image of defects of the first layer after changing the spot size c) In-situ image of defects of the second layer d) In-situ image of defects after single powder layer recoating.

energy distribution and melt pool morphology vary depending on the changes in beam size. Changing the spot size by defocusing the laser at the powder surface level spreads the given amount of energy over a larger surface area. As the laser melts the powder, the high energy creates overheating, meaning a larger and deeper, and hence, possibly unstable melt pool and keyhole pores. An unstable melt pool may yield a spatter of a fraction of the melt pool, which results in fabricating parts with low quality and poor mechanical properties. In this experiment, some good layers were first built using the optimized process parameters, and afterwards the operator stopped the process, changed the laser beam diameter from 100 μm to 150 μm, and started the system to continue creating a new layer. The rest of the process parameters were kept constant. The laser beam size on the surface of the build was changed by altering the focal point position on the powder surface level. To change the focal point position, the computer controller of the laser was used through which the operator could manage the focal point position. The reason for the deliberate change in laser beam diameter was forcing the system to create a defect in the layer under development in order to check whether the in-situ monitoring algorithm was capable of running the image processing on each image of the deposited layer and detecting the defect in that specific layer. As designed, the monitoring system was capturing an image after each layer was forming. Fig. 12a shows the image of the latest completed layer before changing the laser beam diameter. When the laser spot diameter was changed, the monitoring system took an image of the defective layer. The image processing algorithm was able to successfully detect

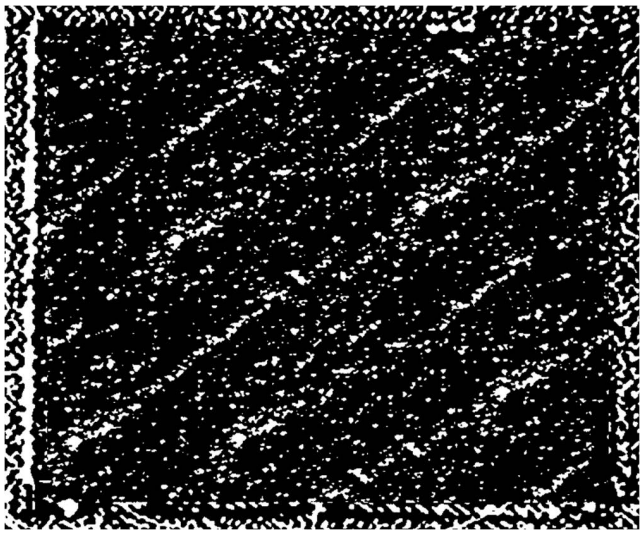

FIGURE 13. Layer surface after changing the layer thickness from 20 μm to 15 μm.

the error and stop the process. Defect alarm was also sent to the UI to notify the operator. The machine was then started again manually by the operator to monitor the processing of all layers. Creating more layers on top of the previous layers with the wrong focal point continued to monitor the build quality of several layers with unoptimized focal point. Fig. 12b-d illustrate the defects of layers after altering the laser spot diameter. The images were taken after a layer was totally processed before the next layer was deposited and processed.

As illustrated in Fig. 12a, when the focal point was in its optimal position and the size of the laser beam on the layer and thus the energy emitted by the laser beam was optimized, the fused layers were created with good quality. Each fused powder line was very symmetrical and there was no hot spot, spatter, or uneven melting pool. As soon as the focal point changed from the optimal size and position, defects appeared in the layer under creation, as shown in Fig. 12b, Fig. 12c, and Fig. 12d. The fused layer was uneven, and the melting pool suffered from the extra energy applied to the molten metal particles. Also, fused lines were no longer visible. As can be seen in Fig. 12b and Fig. 12c, the quality of the layer deteriorated layer by layer and hot spots appeared throughout the second layer. Even after the new powder layer covered the second layer, some areas of the previous layer were not coated by the new metal powder layer due to spatters and uneven melted surface.

B. DEFECT OF POWDER LAYER THICKNESS

Although this subject has been reported intensively in early publications and is commonly applied in many commercial SLM machines, it was still reasonable to be investigated in order to examine the monitoring system and the algorithm designed in this research, and also to study the impact of changing the powder layer thickness on the melting pool and quality of the build. The layer thickness at the point where the interaction occurs between the laser beam and the powder is influential. Layer thickness defect influences the energy density, penetration depth, and consequently bonding between the layers, and the whole process gets involved in resolving the thickness defect. It causes inter-layer porosity, which leads to poor density and mechanical properties of the component. Also, layer thickness is a contributing parameter in causing geometric inaccuracy and dimensional deviations [31]. The thinner powder layer absorbs higher energy, which results in kinetic densification and consolidation. However, if the powder thickness is not enough, balling effect or other track defects can happen.

In this experiment, the uneven thickness of the powder on the platform caused a deliberate defect. Two different methods were used to intentionally apply the defect in the build. In the first method, the software that was controlling the SLM machine was used by the operator to change the thickness of the powder manually. The thickness of the initial layer was changed from 20 μm to 15 μm in the computer controller of the laser and the rest of parameters were kept unchanged to check the effect of the layer thickness on the quality of surface. The image acquired by the monitoring system illustrated in Fig. 13 showed that the melting process was affected by decreasing the powder thickness. By reducing the powder thickness to 15 μm, higher energy was absorbed, which led to the spatter formation on the melt pool, as observed in Fig. 13.

In the second method, the process was stopped in the middle of forming the layer and the thickness of the powder layer was changed by randomly adding/removing powder to/from a part of the surface by the operator. Then the machine was started again to continue creating a new layer. Fig. 14 a) shows the layer surface before applying layer thickness inequality, while Fig. 14 b) illustrates dispersion of heterogeneous powder before starting the SLM process. After starting the process, the monitoring system succeeded in detecting the error based on the captured image and stopped the machine accordingly. However, in order to monitor the formation of more sequential layers with the defective uneven powder layer thickness, the machine was started again manually. This occurred for each layer. Fig. 14 c), d), e) display the in-situ images of the first, second, and third layer of the cube surface formed by the SLM process after applying the thickness defect, which resulted in a different surface thickness of the cube. Similar to Figure 12, the images in Figure 14 were taken after one layer melted and the next layer was deposited.

As revealed by the images, the defect is clearly visible at the left edge of the cube surface of all treated layers. Those areas of the powder layer that were not touched show acceptable quality since the energy density was proper for fusing that thickness of the powder. In areas where the powder layer was not enough, the hot spot appeared, and the melting pool suffered from the extra energy applied to the powder. As shown by the in-situ images, although the defect of the third layer was relatively small, the monitoring system was able to recognize the error and cease the process.

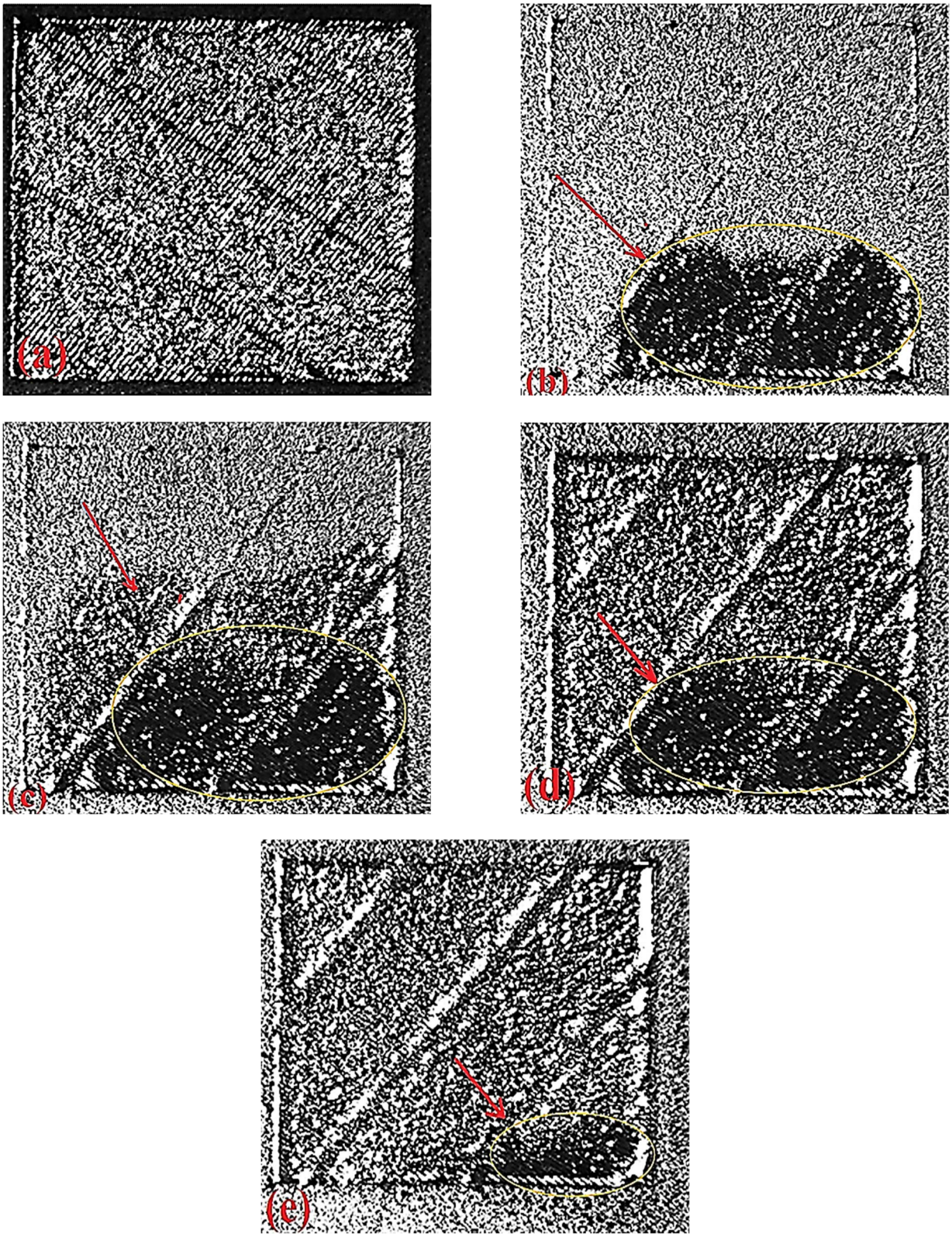

FIGURE 14. a) Layer surface before applying thickness inequality b) Dispersion of heterogeneous powder before starting the SLM process c) In-situ image of the first layer of the cube surface formed by SLM process after applying the thickness defect d) In-situ image of the second layer of the cube surface formed by SLM process after applying the thickness defect e) In-situ image of the third layer of the cube surface formed by SLM process after applying the thickness defect.

V. CONCLUSION

In this study, the experiment was conducted to assess the effect of laser process parameters on the object produced by SLM technology from EOS stainless steel 316 L. Also, an in-situ monitoring platform was developed to detect the defects in AM process. SLM system developed for this research includes AM machine equipped with laser system based on fiber laser, camera, illumination system, and powerful industrial computer equipped with Cameral Link Adapter, FPGA, and Real-Time (RT) modules. Different cube samples were made using various laser process parameters. Images were taken utilizing microscopy imaging technique. The structure, scan strategy, and melting feature of all samples were evaluated. Porosity formation and its dependency on factors such as overlapping of tracks were investigated by varying the hatch distance between successive build experiments. Also, a hardness test was performed for all constructed samples. It was concluded that scanning speed and hatch distance significantly influence the hardness of the product.

An in-situ monitoring platform was developed for the SLM process, and its performance was evaluated with experimental method. The experiment was conducted by monitoring the mechanism of melting and solidifying metal powder layer by layer to ensure the defects can be detected in any fused layer in the earliest possible stage of the process before influencing the properties of the final parts. For this purpose, using LabVIEW system design software, an algorithm was designed based on Particle Analysis (PA) to cease the process in the event of detection of any defect and send an alarm to the UI to inform the operator about the defect. As the waiting time for any defect that naturally appears was too long, two types of defects were caused intentionally to evaluate the performance of the platform. The first defect was caused by changing the laser spot diameter with keeping the rest of the parameters constant, and the second defect occurred due to unevenness in the thickness of metal powder. For both cases, the monitoring system appropriately detected the defect and ceased the operation. However, in order to monitor the process for the next layers, the machine was started manually, and the monitoring platform continued controlling the quality of the new layers again. The images were taken online by a high-performance camera layer by layer after creating each defect. It was observed that the systems operated effectively to detect even minor defects and stopped the process accordingly. Microcracks and porosities up to 10 μm can be identified by the developed monitoring platform.

Temperature changes and heat flow during the process impress the solidification morphology in tracks. The future research direction will be observing the temperature variations that occur by laser parameter changes and analyzing the solidification morphology of tracks. Conducting more intensive image processing on this process is another research plan.

REFERENCES

[1] B. Berman, "3-D printing: The new industrial revolution," *Bus. Horizons*, vol. 55, no. 2, pp. 155–162, 2012, doi: 10.1016/j.bushor.2011.11.003.

[2] R. D'Aveni, "The 3-D printing revolution," *Harv. Bus. Rev.*, vol. 93, no. 5, pp. 40–48, May 2015.

[3] W. Gao, Y. Zhang, D. Ramanujan, K. Ramani, Y. Chen, C. B. Williams, C. C. Wang, Y. C. Shin, S. Zhang, and P. D. Zavattieri, "The status, challenges, and future of additive manufacturing in engineering," *Comput.-Aided Des.*, vol. 69, pp. 65–89, Dec. 2015, doi: 10.1016/j.cad.2015.04.001.

[4] M. Attaran, "The rise of 3-D printing: The advantages of additive manufacturing over traditional manufacturing," *Bus. Horizons*, vol. 60, no. 5, pp. 677–688, Sep. 2017, doi: 10.1016/j.bushor.2017.05.011.

[5] H. G. Lemu and S. Kurtovic, "3D printing for rapid manufacturing: Study of dimensional and geometrical accuracy," in *Proc. IFIP Int. Conf. Adv. Prod. Manage. Syst.*, vol. 384, J. Frick and B. T. Laugen, Eds. Berlin, Germany: Springer, Jan. 2012, pp. 470–479, doi: 10.1007/978-3-642-33980-6_51.

[6] I. Gibson, D. Rosen, and B. Stucker, *Additive Manufacturing Technologies*, 2nd ed. New York, NY, USA: Springer, 2015.

[7] A. A. Albarnawi and M. O. Bashir, "Additive manufacturing: A new industrial revolution—A review," *J. Sci. Achiev.*, vol. 2, no. 3, pp. 19–31, Mar. 2017.

[8] Y. Qin, Q. Qi, P. J. Scott, and X. Jiang, "Status, comparison, and future of the representations of additive manufacturing data," *Comput.-Aided Des.*, vol. 111, pp. 44–64, Jun. 2019, doi: 10.1016/j.cad.2019.02.004.

[9] A. H. Azman, F. Vignat, and F. Villeneuve, "Cad tools and file format performance evaluation in designing lattice structures for additive manufacturing," *Jurnal Teknologi*, vol. 80, no. 4, pp. 87–95, Apr. 2018, doi: 10.11113/jt.v80.12058.

[10] N. Shahrubudin, T. C. Lee, and R. Ramlan, "An overview on 3D printing technology: Technological, materials, and applications," *Proc. Manuf.*, vol. 35, pp. 1286–1296, Jan. 2019, doi: 10.1016/j.promfg.2019.06.089.

[11] V. Sharma, H. Roozbahani, M. Alizadeh, and H. Handroos, "3D printing of plant-derived compounds and a proposed nozzle design for the more effective 3D FDM printing," *IEEE Access*, vol. 9, pp. 57107–57119, 2021, doi: 10.1109/ACCESS.2021.3071459.

[12] M. Revilla-León, M. J. Meyer, and M. Özcan, "Metal additive manufacturing technologies: Literature review of current status and prosthodontic applications," *Int. J. Comput. Dent.*, vol. 22, no. 1, pp. 55–67, 2019.

[13] D. Herzog, V. Seyda, E. Wycisk, and C. Emmelmann, "Additive manufacturing of metals," *Acta Mater.*, vol. 117, pp. 371–392, Sep. 2016, doi: 10.1016/j.actamat.2016.07.019.

[14] W. E. Frazier, "Metal additive manufacturing: A review," *J. Mater. Eng. Perform.*, vol. 23, no. 6, pp. 1917–1928, 2014, doi: 10.1007/s11665-014-0958-z.

[15] S. L. Sing, C. N. Kuo, C. T. Shih, C. C. Ho, and C. K. Chua, "Perspectives of using machine learning in laser powder bed fusion for metal additive manufacturing," *Virtual Phys. Prototyping*, vol. 16, no. 3, pp. 372–386, Jul. 2021, doi: 10.1080/17452759.2021.1944229.

[16] Y. Qin, Q. Qi, P. Shi, P. J. Scott, and X. Jiang, "Automatic determination of part build orientation for laser powder bed fusion," *Virtual Phys. Prototyping*, vol. 16, no. 1, pp. 29–49, Jan. 2021, doi: 10.1080/17452759.2020.1832793.

[17] S. L. Sing, S. Huang, G. D. Goh, G. L. Goh, C. F. Tey, J. H. K. Tan, and W. Y. Yeong, "Emerging metallic systems for additive manufacturing: *in-situ* alloying and multi-metal processing in laser powder bed fusion," *Prog. Mater. Sci.*, vol. 119, Jun. 2021, Art. no. 100795, doi: 10.1016/j.pmatsci.2021.100795.

[18] C. Y. Yap, C. K. Chua, Z. L. Dong, Z. H. Liu, D. Q. Zhang, L. E. Loh, and S. L. Sing, "Review of selective laser melting: Materials and applications," *Appl. Phys. Rev.*, vol. 2, no. 4, Dec. 2015, Art. no. 041101, doi: 10.1063/1.4935926.

[19] J. A. Slotwinski, E. J. Garboczi, and K. M. Hebenstreit, "Porosity measurements and analysis for metal additive manufacturing process control," *J. Res. Nat. Inst. Standards Technol.*, vol. 119, pp. 494–528, Sep. 2014, doi: 10.6028/jres.119.019.

[20] M. Van Elsen, "Complexity of selective laser melting: A new optimisation approach," Ph.D. dissertation, Dept. Prod. Techn., K. U. Leuven, Brussels, Belgium, 2007.

[21] I. Yadroitsev, P. Krakhmalev, I. Yadroitsava, S. Johansson, and I. Smurov, "Energy input effect on morphology and microstructure of selective laser melting single track from metallic powder," *J. Mater. Process. Technol.*, vol. 213, no. 4, pp. 606–613, Apr. 2013, doi: 10.1016/j.jmatprotec.2012.11.014.

[22] H. Gu, H. Gong, D. Pal, K. H. Rafi, T. Starri, and B. Stucher, "Influences of energy density on porosity and microstructure of selective laser melted 17-4PH stainless steel," in *Proc. 24th Int. SFF Symp. Additive Manuf. Conf.*, Aug. 2013, pp. 1–16.

[23] O. A. Mohamed, S. H. Masood, and W. Xu, "Nickel-titanium shape memory alloys made by selective laser melting: A review on process optimisation," *Adv. Manuf.*, vol. 10, no. 1, pp. 24–58, Jan. 2022, doi: 10.1007/s40436-021-00376-9.
[24] S. L. Sing, "Perspectives on additive manufacturing enabled Beta- titanium alloys for biomedical applications," *Int. J. Bioprinting*, vol. 8, no. 1, p. 478, Jan. 2022, doi: 10.18063/ijb.v8i1.478.
[25] F. Rivalta, L. Ceschini, A. E. W. Jarfors, and R. Stolt, "Effect of scanning strategy in the L-PBF process of 18Ni300 maraging steel," *Metals*, vol. 11, no. 5, p. 826, May 2021, doi: 10.3390/met11050826.
[26] S. Huang, R. L. Narayan, J. H. K. Tan, S. L. Sing, and W. Y. Yeong, "Resolving the porosity-unmelted inclusion dilemma during *in-situ* alloying of Ti34Nb via laser powder bed fusion," *Acta Mater.*, vol. 204, Feb. 2021, Art. no. 116522, doi: 10.1016/j.actamat.2020.116522.
[27] H. Roozbahani, P. Marttinen, and A. Salminen, "Real-time monitoring of laser scribing process of CIGS solar panels utilizing high-speed camera," *IEEE Photon. Technol. Lett.*, vol. 30, no. 20, pp. 1741–1744, Oct. 15, 2018, doi: 10.1109/LPT.2018.2867274.
[28] H. Roozbahani, A. Salminen, and M. Manninen, "Real-time online monitoring of nanosecond pulsed laser scribing process utilizing spectrometer," *J. Laser Appl.*, vol. 29, no. 2, May 2017, Art. no. 022208, doi: 10.2351/1.4983520.
[29] P. Yadav, O. Rigo, C. Arvieu, E. Le Guen, and E. Lacoste, "*In situ* monitoring systems of the SLM process: On the need to develop machine learning models for data processing," *Crystals*, vol. 10, no. 6, p. 524, Jun. 2020, doi: 10.3390/cryst10060524.
[30] P. Lott, H. Schleifenbaum, W. Meiners, K. Wissenbach, C. Hinke, and J. Bültmann, "Design of an optical system for the *in situ* process monitoring of selective laser melting (SLM)," *Phys. Proc.*, vol. 12, pp. 683–690, Jan. 2011, doi: 10.1016/j.phpro.2011.03.085.
[31] B. Zhang, Y. Li, and Q. Bai, "Defect formation mechanisms in selective laser melting: A review," *Chin. J. Mech. Eng.*, vol. 30, no. 3, pp. 515–527, Apr. 2017, doi: 10.1007/s10033-017-0121-5.
[32] A. Maamoun, Y. Xue, M. Elbestawi, and S. Veldhuis, "Effect of selective laser melting process parameters on the quality of al alloy parts: Powder characterization, density, surface roughness, and dimensional accuracy," *Materials*, vol. 11, no. 12, p. 2343, Nov. 2018, doi: 10.3390/ma11122343.
[33] P. Bajaj, J. Wright, I. Todd, and E. A. Jägle, "Predictive process parameter selection for selective laser melting manufacturing: Applications to high thermal conductivity alloys," *Additive Manuf.*, vol. 27, pp. 246–258, May 2019, doi: 10.1016/j.addma.2018.12.003.
[34] S. Greco, K. Gutzeit, H. Hotz, B. Kirsch, and J. C. Aurich, "Selective laser melting (SLM) of AISI 316L—Impact of laser power, layer thickness, and hatch spacing on roughness, density, and microhardness at constant input energy density," *Int. J. Adv. Manuf. Technol.*, vol. 108, nos. 5–6, pp. 1551–1562, May 2020, doi: 10.1007/s00170-020-05510-8.
[35] S. Barua, F. Liou, J. Newkirk, and T. Sparks, "Vision-based defect detection in laser metal deposition process," *Rapid Prototyping J.*, vol. 20, no. 1, pp. 77–85, Jan. 2014, doi: 10.1108/RPJ-04-2012-0036.
[36] G. Tapia and A. Elwany, "A review on process monitoring and control in metal-based additive manufacturing," *J. Manuf. Sci. Eng.*, vol. 136, no. 6, Dec. 2014, Art. no. 060801, doi: 10.1115/1.4028540.
[37] M. Grasso, V. Laguzza, Q. Semeraro, and B. M. Colosimo, "In-process monitoring of selective laser melting: Spatial detection of defects via image data analysis," *J. Manuf. Sci. Eng.*, vol. 139, no. 5, pp. 1–16, Nov. 2016, doi: 10.1115/1.4034715.
[38] E. Malekipour and H. El-Mounayri, "Common defects and contributing parameters in powder bed fusion AM process and their classification for online monitoring and control: A review," *Int. J. Adv. Manuf. Technol.*, vol. 95, nos. 1–4, pp. 527–550, Mar. 2018, doi: 10.1007/s00170-017-1172-6.
[39] B. Lane, E. Whitenton, and S. Moylan, "Multiple sensor detection of process phenomena in laser powder bed fusion," *Proc. SPIE*, vol. 9861, pp. 20–28, May 2016, doi: 10.1117/12.2224390.
[40] A. G. Demir, C. D. Giorgi, and B. Previtali, "Design and implementation of a multisensor coaxial monitoring system with correction strategies for selective laser melting of a maraging steel," *J. Manuf. Sci. Eng.*, vol. 140, no. 4, pp. 1–51, Feb. 2018, doi: 10.1115/1.4038568.
[41] A. Remani, R. Williams, A. Thompson, J. Dardis, N. Jones, P. Hooper, and R. Leach, "Design of a multi-sensor measurement system for *in-situ* defect identification in metal additive manufacturing," in *Proc. Euspen/ASPE Advancing Precision Additive Manuf.*, St. Gallen, Switzerland, Sep. 2021, pp. 1–4.
[42] L. Song, W. Huang, X. Han, and J. Mazumder, "Real-time composition monitoring using support vector regression of laser-induced plasma for laser additive manufacturing," *IEEE Trans. Ind. Electron.*, vol. 64, no. 1, pp. 633–642, Jan. 2017, doi: 10.1109/TIE.2016.2608318.
[43] J. L. Bartlett, F. M. Heim, Y. V. Murty, and X. Li, "*In situ* defect detection in selective laser melting via full-field infrared thermography," *Additive Manuf.*, vol. 24, pp. 595–605, Dec. 2018, doi: 10.1016/j.addma.2018.10.045.
[44] D. Ye, G. S. Hong, Y. Zhang, K. Zhu, and J. Y. H. Fuh, "Defect detection in selective laser melting technology by acoustic signals with deep belief networks," *Int. J. Adv. Manuf. Technol.*, vol. 96, nos. 5–8, pp. 2791–2801, May 2018, doi: 10.1007/s00170-018-1728-0.
[45] T. Liu, L. Huang, and B. Chen, "Real-time defect detection of laser additive manufacturing based on support vector machine," *J. Phys. Conf. Ser.*, vol. 1213, Jun. 2019, Art. no. 052043, doi: 10.1088/1742-6596/1213/5/052043.
[46] M. Modaresialam, "Real time monitoring of additive manufacturing," M.S. thesis, Dept. Mech. Eng., LUT Mech. Eng., Lappeenranta-Lahti Univ. Technol., Lappeenranta, Finland, 2017.
[47] (2014). *EOS Stainless Steel 316L Material Data Sheet*. Accessed: Jul. 19, 2021. [Online]. Available: https://www.eos.info/03_system-related-assets/material-related-contents/metal-materials-and-examples/metal-material-datasheet/stainlesssteel/material_datasheet_eos_stainlesssteel_316l_en_web.pdf
[48] (2015). *Technical Description EOSINT M 270 Machine*. Accessed: Jul. 19, 2021. [Online]. Available: https://www.nobilium.com/skin/frontend/ultimo/default/pdf/TD_M270_Dental-Package_10-15_en.pdf
[49] Y. Lu, S. Wu, Y. Gan, T. Huang, C. Yang, L. Junjie, and J. Lin, "Study on the microstructure, mechanical property and residual stress of SLM inconel-718 alloy manufactured by differing island scanning strategy," *Opt. Laser Technol.*, vol. 75, pp. 197–206, Dec. 2015, doi: 10.1016/j.optlastec.2015.07.009.
[50] D. Dai, D. Gu, H. Zhang, J. Xiong, C. Ma, C. Hong, and R. Poprawe, "Influence of scan strategy and molten pool configuration on microstructures and tensile properties of selective laser melting additive manufactured aluminum based parts," *Opt. Laser Technol.*, vol. 99, pp. 91–100, Feb. 2018, doi: 10.1016/j.optlastec.2017.08.015.
[51] I. Rosenthal, A. Stern, and N. Frage, "Microstructure and mechanical properties of AlSi10Mg parts produced by the laser beam additive manufacturing (AM) technology," *Metallography, Microstruct., Anal.*, vol. 3, no. 6, pp. 448–453, Dec. 2014, doi: 10.1007/s13632-014-0168-y.
[52] F. Trevisan, F. Calignano, M. Lorusso, J. Pakkanen, A. Aversa, and P. E. Ambrosio, "On the selective laser melting (SLM) of the AlSi10Mg alloy: Process, microstructure, and mechanical properties," *Materials*, vol. 10, no. 76, pp. 1–23, Jan. 2017, doi: 10.3390/ma10010076.
[53] C. U. Brown, G. A. Jacob, A. Possolo, C. Beauchamp, M. A. Peltz, M. R. Stoudt, and A. M. Donmez, "The effects of laser powder bed fusion process parameters on material hardness and density for nickel alloy 625," in *Advanced Manufacturing Series (NIST AMS)*. Gaithersburg, MD, USA: National Institute of Standards and Technology, doi: 10.6028/NIST.AMS.100-19.
[54] C. Kamath, B. El-Dasher, G. F. Gallegos, W. E. King, and A. Sisto, "Density of additively-manufactured, 316L SS parts using laser powder-bed fusion at powers up to 400 W," *Int. J. Adv. Manuf. Technol.*, vol. 74, nos. 1–4, pp. 65–78, 2014, doi: 10.1007/s00170-014-5954-9.

MEHRNAZ MODARESIALAM received the M.Sc. degree in technical physics (computational engineering) from Lappeenranta-Lahti University of Technology, Finland, and the double M.Sc. degree in nanoscience and nanotechnology from Université Grenoble Alpes. She is currently pursuing the Ph.D. degree with Aix-Marseille University. Her main research work was the development of laser and optical systems for additive manufacturing machines and quality control of final products. Her research interests include material science, nanofabrication, metal oxides, dielectric materials, and the development of optical performances for different industrial applications: photovoltaic and gas sensors.

HAMID ROOZBAHANI (Member, IEEE) received the Master of Science and D.Sc.Tech. degrees in mechatronics from the Lappeenranta-Lahti University of Technology. For several years, he has been working as a Project Manager in several projects starting, since 1999. Currently, he is serving as a Research Scientist, a Project Manager, and a Lecturer with the Lappeenranta-Lahti University of Technology. He is also a Project Manager of EU funded project APPOLO and TIERA—LUT Mobile Robot Project.

MARJAN ALIZADEH received the B.Sc. degree in electrical engineering (control) from the Ferdowsi University of Mashhad, Iran, in 2003, and the M.Sc. degree in electrical engineering (industrial electronics) from the Lappeenranta-Lahti University of Technology, Finland, in 2017. From 2003 to 2015, she was working in the field of electrical engineering in industry. Currently, she is working as a Project Researcher with the Lappeenranta-Lahti University of Technology.

ANTTI SALMINEN is currently a Professor in mechanical engineering with the University of Turku and a Docent in manufacturing technology with LUT University. He has more than 30 years of experience of laser-based manufacturing processes and welding in both academia and industry. He has been a Principal Investigator in several research projects funded by the National, Nordic, and European funding agents. He has published more 100 peer reviewed scientific and more than 150 scientific conference publications. He has supervised ten doctoral, 70 master's, and 16 bachelor's theses. He is currently supervising eight doctoral theses. His research interests include the process and laser system development, product design utilizing laser processing, and additive manufacturing and monitoring of thermal processes, especially for welding and additive manufacturing. He is a Member of Board of the Finnish Association for Additive Manufacturing and a Deputy Member of Board of the Finnish Welding Society and National Delegate in IIW Commissions I, IV, and X.

HEIKKI HANDROOS (Member, IEEE) received the D.Sc. (Tech.) degree from the Tampere University of Technology. He has been a Professor of machine automation with the Lappeenranta-Lahti University of Technology, since 1992. He has been a Visiting Professor with the University of Minnesota; Peter the Great St.Petersburg Polytechnic University; and the National Defense Academy, Japan. He has published about 250 international scientific papers and supervised around 20 D.Sc. theses. He has held several positions of trust in American Society of Mechanical Engineers. He has led several important domestic and international research projects. His research interests include modeling, design, and control of mechatronic transmissions to robotics and virtual engineering.